Magnetically-refreshable receptor platform structures for reusable nano-biosensor chips

2016 Nanotechnology 27 045502

(http://iopscience.iop.org/0957-4484/27/4/045502)

IOP Publishing Nanotechnology
Nanotechnology 27 (2016) 045502 (10pp) doi:10.1088/0957-4484/27/4/045502

Magnetically-refreshable receptor platform structures for reusable nano-biosensor chips

Haneul Yoo[1], Dong Jun Lee[2], Dong-guk Cho[1], Juhun Park[1], Ki Wan Nam[1], Young Tak Cho[1], Jae Yeol Park[3], Xing Chen[1,4] and Seunghun Hong[1]

[1] Department of Physics and Astronomy, and Institute of Applied Physics, Seoul National University, Seoul 151-747, Korea
[2] Department of Biophysics and Chemical Biology, Seoul National University, Seoul 151-742, Korea
[3] Department of Automotive Engineering, Doowon Technical University College, Anseong 456-718, Korea
[4] Research Center for Biomimetic Functional Materials and Sensing Devices, Institute of Intelligent Machines, Chinese Academy of Sciences, Hefei 230031, People's Republic of China

E-mail: shong@phya.snu.ac.kr

Received 30 September 2015, revised 17 November 2015
Accepted for publication 20 November 2015
Published 14 December 2015

Abstract

We developed a magnetically-refreshable receptor platform structure which can be integrated with quite versatile nano-biosensor structures to build *reusable* nano-biosensor chips. This structure allows one to easily remove used receptor molecules from a biosensor surface and reuse the biosensor for repeated sensing operations. Using this structure, we demonstrated reusable immunofluorescence biosensors. Significantly, since our method allows one to place receptor molecules very close to a nano-biosensor surface, it can be utilized to build reusable carbon nanotube transistor-based biosensors which require receptor molecules within a Debye length from the sensor surface. Furthermore, we also show that a single sensor chip can be utilized to detect two different target molecules simply by replacing receptor molecules using our method. Since this method does not rely on any chemical reaction to refresh sensor chips, it can be utilized for versatile biosensor structures and virtually-general receptor molecular species.

S Online supplementary data available from stacks.iop.org/NANO/27/045502/mmedia

Keywords: single-layered, magnetic trapping-detrapping, reusable biosensor, fluorescence, carbon nanotube field-effect transistor

(Some figures may appear in colour only in the online journal)

1. Introduction

Biosensors are a key component for versatile analytical applications such as disease diagnosis [1–9], drug screening [10], environmental monitoring [11], and bioterrorism prevention [12]. Until now, most conventional biosensors have been manufactured as a disposable chip only for a one-time use. However, for various applications, one needs to use a single biosensor chip for repeated sensing operations. For example, recent progress of nano-biotechnology enabled various advanced nano-biosensors such as carbon nanotube (CNT) transistor-based biosensors [13], nanowire-based biosensors [14], and magnetic beads-based biosensors [15]. Such nano-biosensors take advantage of the superior characteristics of nano-devices [16] and exhibit high performances such as a high sensitivity and a fast response time. However, one of the major hurdles holding back their practical applications can be the rather high cost of such nano-devices [17]. Thus, a strategy to reuse a single nano-biosensor chip for repeated sensing operations can be a key stepping stone to bring such high-performance, but expensive, nano-biosensors toward practical applications. On the other hand, there have been extensive efforts to develop an alarming system which can be installed in a public place (e.g. airport) and used to

monitor hazardous viruses or bioterror substances in the air for a long time period [18, 19]. For such applications, one needs a reusable biosensor device which can be utilized repeatedly over a long time period without being replaced. Extensive efforts have been made to develop reusable nano-biosensor chips using various methods such as the chemical refreshment of receptors, magnetic bead-based methods etc [20–26]. However, previous methods often leave chemical contaminations or thick layers of receptors on sensor chip surfaces, limiting their applications only for some specific receptor molecules or sensor structures.

Herein, we report a magnetically-refreshable receptor platform (MRP) structure which can be integrated with virtually-general nano-biosensor structures to build *reusable* nano-biosensor chips. The hysteresis properties of ferromagnetic MRP structures integrated with a nano-biosensor were utilized to generate *attractive* or *repulsive* forces between receptor-functionalized magnetic nanobeads and the ferromagnetic MRP structures under external magnetic fields, so that one can *trap* or *remove* receptors on the nano-biosensor, respectively. Thus, one can easily remove used receptor molecules on the nano-biosensor surface and place new receptors with a controlled thickness for repeated sensing operations. Furthermore, since the residual magnetization of the ferromagnetic MRP structures can hold receptor-functionalized nanobeads on the sensor surfaces without external magnetic fields, the sensors can be used for versatile applications such as imaging analyses and sensing operations in a conventional manner without external magnetic fields. The MRP structure was successfully utilized to build reusable immunofluorescence biosensor chips for repeated sensing operations while maintaining its sensitivity and selectivity. Significantly, since, in this method, receptor-functionalized nanoparticles form single-layered film structures without stacking as multiple layers on the MRP structures, one can place receptors close to the nano-biosensor surfaces. Note that some nano-biosensor structures such as transistor-based electrical biosensors require receptor molecules close to sensor surfaces for sensing operations. We successfully integrated the MRP structures with CNT transistor structures to build reusable biosensor chips. The MRP structure is a simple but versatile structure which can be applied for quite versatile nano-biosensor structures and virtually-general receptor molecules to build reusable biosensor chips. Thus, it can be a major breakthrough which can bring rather expensive nano-biosensors for practical applications and may even enable new bio-analysis applications such as the monitoring of hazardous biological entities in public places.

2. Experimental methods

2.1. Preparation of antibody-functionalized nanobeads, fluorescence-labeled capture antibody, and antigens

Human interleukins (IL-4, IL-10), their biotinylated detection antibody (labeled as 1st antibody), capture antibody (labeled as 2nd antibody) and an antigen were purchased from eBioscience company (USA). Streptavidin-coated pink-fluorescent superparamagnetic nanobeads (Nano-screen-MAG-Streptavidin, with its hydrodynamic diameter of 100 nm, 1 mg ml^{-1} in phosphate buffered saline (PBS) solution) were purchased from Chemicell GmbH (Germany). Fluorescein isothiocyanate (FITC), Poly(ethylene glycol) thiol (PEG-SH, MW 5000) and other chemical reagents were purchased from Sigma-Aldrich (USA). To prepare nanobeads functionalized with the 1st antibody, 100 μl solution of the streptavidin-coated superparamagnetic nanobeads (1 mg ml^{-1} in PBS solution) was first mixed with 20 μl solution of the biotinylated 1st antibody (1 mg ml^{-1} in PBS solution), and the mixed solution was incubated at room temperature for 1 h. Finally, it was diluted to 1000 μl in PBS solution. The conjugation of the 2nd antibody with FITC was performed following the procedure of the FluoroTag FITC conjugation kit.

2.2. Experimental procedure for trapping and detrapping of single-layered film structures of fluorescence-labeled nanobeads

A solenoid (custom made, NS Magnet, Korea) was purchased and used for generating external magnetic fields. The solenoid was comprised of 7500 turned electric wires and a 1.5 cm × 6.3 cm cylindrical iron core. For the trapping of fluorescence-labeled nanobeads as a single-layered film structure, 50 μl (1 mg ml^{-1} in PBS solution) of fluorescence-labeled magnetic nanobead solution was placed on MRP structures patterned on a SiO_2 substrate, and an external magnetic field (150 mT) was applied in a perpendicular direction to the substrate for 90 s. After removing the magnetic field, the substrate was washed by PBS solution. For the detrapping of the nanobeads, 35 mT of an external magnetic field in an opposite direction was applied for 10 s, and the substrate was washed by PBS solution. After each trapping and detrapping steps, the amount of the fluorescence-labeled nanobeads assembled on the substrate was measured by a fluorescence microscope (TE2000U, Nikon, Japan) with a rhodamine filter.

2.3. Fabrication of reusable fluorescence biosensors

Ferromagnetic MRP patterns (10 nm Au on 10 nm Ni, 30 × 28 Ni/Au patterns of size 4 μm × 8 μm) were fabricated on a SiO_2 substrate (100 nm-thick SiO_2 film on Si wafer) via conventional microfabrication processes. The substrate with the patterns was immersed in an octadecyltrichlorosilane (OTS) solution (1:500, v/v in hexane) for 5 min and then rinsed thoroughly by anhydrous hexane. Here, a self-assembled OTS monolayer formed on the SiO_2 surface passivated the SiO_2 surfaces. Later, the substrate was immersed in a PEG-SH solution (20 mg ml^{-1} in deionized water) for ~10 h at room temperature. In this process, a PEG layer was formed on the Au film over the ferromagnetic nickel-based MRP structures, which minimized the adhesion of biomolecules and nanobeads on the MRP structures.

2.4. Repeated sensing operations of reusable fluorescence biosensors

A 50 μl solution of antibody-functionalized magnetic nanobeads was first placed on a SiO_2 substrate with ferromagnetic MRP structures, and an external magnetic field (150 mT) was applied in a perpendicular direction to the substrate plane for 90 s. In this step, a monolayer of antibody-functionalized nanobeads was assembled on the ferromagnetic MRP structures so that the antibody molecules on the nanobeads could be utilized for a biosensing operation. The assembly of nanobeads was confirmed by observing the fluorescence from the nanobeads via a fluorescence microscope. For a complementary sensing operation, the 50 μl solution of a complementary antigen (1 ng ml^{-1} $\approx$ 57.1 pM in PBS solution) was placed on the substrate with assembled nanobeads for 1 h at room temperature and then washed thoroughly with PBS solution. Subsequently, the substrate was incubated with FITC-2nd antibody at room temperature for 1 h. Finally, the selective detection of the antigen was confirmed by observing the fluorescence from FITC-2nd antibodies on the ferromagnetic MRP structures via a fluorescence microscope. After one sensing operation, 35 mT of an external magnetic field was applied in an opposite direction for 10 s, which removed the magnetic nanobeads from the MRP structures. Following this, the solution on the substrate was washed away with clean PBS solution, leaving clean substrate surfaces for additional sensing operations.

2.5. Fabrication of reusable carbon nanotube-based electrical biosensors with ferromagnetic MRP structures

Purified semiconducting single-walled CNTs (swCNT) were purchased from NanoIntegris Inc. (USA) and used as received. The CNTs had a diameter of 0.7–2 nm and a length of 2–3 μm. A CNT transistor with floating electrodes could be fabricated following the method reported previously [27]. At first, the 'surface-programmed assembly' method was used to pattern swCNT network channels on a SiO_2 substrate. Briefly, the patterns of the photoresist layer (AZ5214) were first prepared on the SiO_2 substrate via conventional photolithography, and the substrate was placed in the solution of OTS (1:500, v/v in hexane) for 5 min at room temperature so that the self-assembled monolayer (SAM) of OTS was formed on the bare SiO_2 surface. Later, the substrate was rinsed with clean anhydrous hexane, acetone, and ethanol in sequence, leaving OTS SAM patterns and bare SiO_2 surface regions. The substrate is placed in the CNT solution (0.1 mg ml^{-1} in 1,2-dichlorobenzene) for 30 s so that CNTs in the solution were selectively adsorbed onto the bare SiO_2 surface regions and formed CNT network channels. The wafer was rinsed thoroughly with 1,2-dichlorobenzene and dried with nitrogen gas. In this work, we prepared swCNT channels with its width of 3 μm. The source and drain electrodes (30 nm Au on 10 nm Ti), and the five floating electrodes (10 nm Au on 10 nm Ni) were fabricated via conventional photolithography, thermal evaporation, and lift-off processes. Following this, the source and drain electrodes were covered with a photoresist layer (DNR-L300-30) to passivate the electrodes. The fabricated devices were immersed in the PEG-SH solution (20 mg ml^{-1} in deionized water) overnight and washed with deionized water so that PEG layer was formed on the floating electrodes and minimized the non-specific adsorption of biomolecules during biosensing experiments. The devices were also immersed in the TWEEN-20 solution (0.5%) for 10 min and washed by deionized water to passivate the CNT channel surface [27].

2.6. Repeated sensing operations of reusable carbon nanotube transistor-based biosensors

The bio-sensing operations of reusable CNT based biosensors were performed in PBS solution using an Ag/AgCl electrode as a liquid gate electrode. At first, the solution of antibody-functionalized nanobeads (1 mg ml^{-1} in PBS solution) was applied to the CNT device, and an external magnetic field (150 mT) was applied along the vertical direction to the substrate surface for 90 s so that a monolayer of nanobeads were assembled on the surface of the ferromagnetic MRP structure in the floating electrodes. Afterwards, a target molecular solution was applied to the device while monitoring the source-drain current with a source-drain bias of 100 mV and liquid gate bias of -200 mV. The source-drain currents of CNT transistor devices were measured using a semiconductor characterization system (4200-SCS, Keithley, USA). The current change ratio $\Delta I/I_0$ was utilized as a sensing signal.

2.7. Morphological analysis

Atomic force microscopy (AFM) imaging was performed using a commercial AFM system (MFP-3D, Asylum Research) in a tapping mode. A field emission scanning electron microscope (FE-SEM) (Hitachi 4800, Hitachi) was used for the SEM imaging.

3. Results and discussion

Figure 1 shows the schematic diagram showing the repeated sensing operations of a biosensor based on a ferromagnetic MRP structure. Detailed processes are presented in section 2. In brief, an MRP structure based on ferromagnetic nickel thin film patterns was first fabricated as part of a biosensor device in the active sensing regions of the biosensor device so that it can respond to the binding activity of the receptors in the regions (figure 1(A)). Depending on the biosensor structures, the ferromagnetic MRP structures can be integrated in different formations. For example, in the case of transistor-based electrical sensors, the MRP structures can be a part of its electrodes. For a sensing operation, the biosensor was placed in the solution of magnetic nanobeads (orange spheres) functionalized with specific receptor molecules (y-shaped symbols), and external magnetic fields (black dashed arrows) were applied in a perpendicular direction to the MRP structures (figure 1(B)). In the external magnetic fields, the

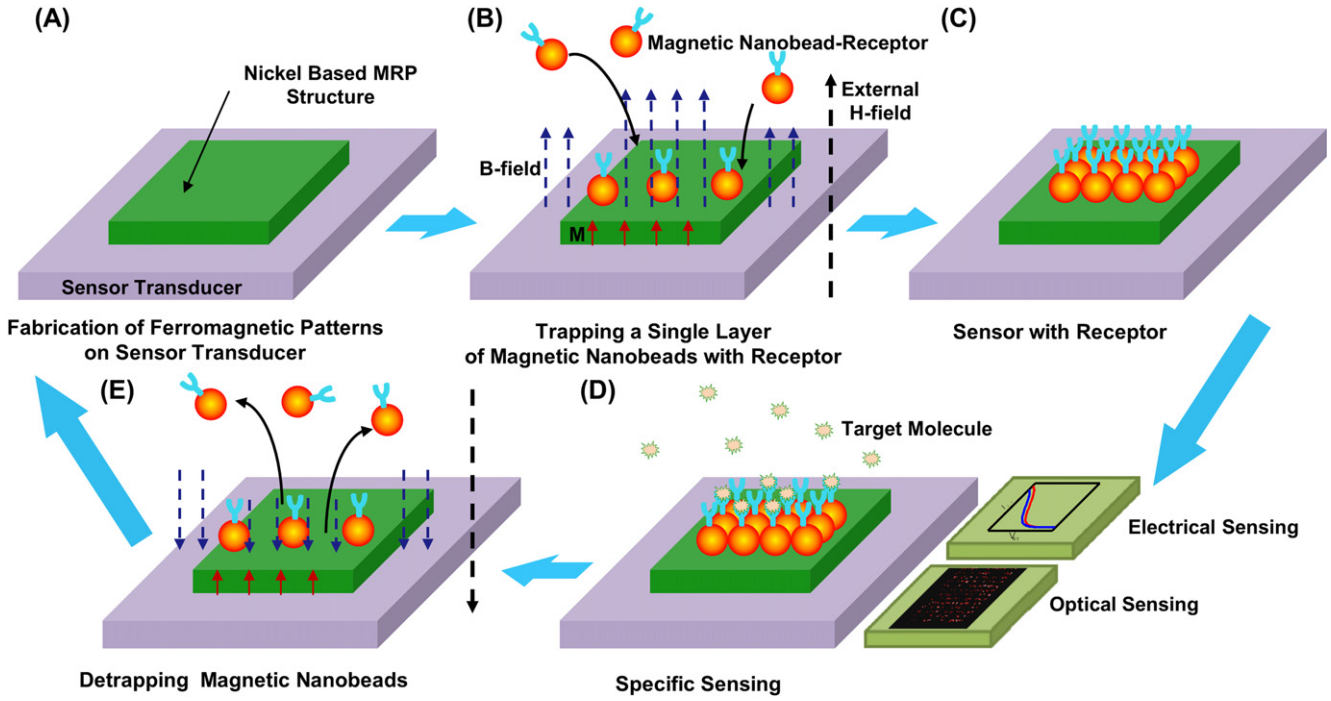

Figure 1. Schematic diagram showing the repeated sensing operations of a reusable nano-biosensor based on an MRP structure. (A) Fabrication of a ferromagnetic MRP structure on a biosensor transducer surface. (B) Trapping of single-layered film structures of magnetic nanobeads functionalized with receptors via a rather strong external magnetic field. A *black dashed arrow, red arrows*, and *blue dashed arrows* represent *an external magnetic field*, *the magnetization of the ferromagnetic MRP structure*, and *total magnetic fields*, respectively. (C) Formation of a single-layered film structure of magnetic nanobeads on the ferromagnetic MRP structure. (D) Sensing operation using the receptor molecules on the assembled nanobeads. (E) Removal of the nanobeads.

ferromagnetic MRP structures were magnetized (red arrows) along the direction of the external fields, and the magnetic fields (blue dashed arrows) just above the pattern became stronger than those in other regions. Thus, the magnetic nanobeads in the solution were attracted toward the MRP structures and formed a layered structure. Here, using ferromagnetic MRP structures with a proper thickness and shape, we could generate strong magnetic field regions only in a very short distance above the structures so that nanobeads formed a single-layered film structure (figure 1(C)). Note that the residual magnetization of the ferromagnetic MRP structures can hold assembled magnetic nanobeads even without any external magnetic fields. Thus, we could take out the MRP structures from the solution environments with external magnetic fields and perform sensing operations in a conventional manner without any external magnetic fields. Since the receptors on the assembled nanobeads were near the biosensor surface, they can be utilized for the selective detection of specific target molecules via the biosensor (figure 1(D)). As a proof of concepts, we demonstrated the repeated sensing operations of biosensors based on fluorescence and CNT transistor measurements. After the sensing operation, a rather weak external magnetic field with a reversed direction was applied *so that the magnetic fields in the solution were reversed while the magnetization of the MRP structures remained* due to the hysteresis of the ferromagnetic materials (figure 1(E)). In this case, since the remaining magnetization of the ferromagnetic MRP structures had an opposite direction to the external magnetic fields, the total magnetic fields just above the MRP structures became weaker than those in other regions. Thus, the magnetic nanobeads were moved away from the MRP structures, and the surface of the sensor transducer was restored to a clean surface (figure 1(A)). By repeating these processes, we could perform repeated sensing operations using a single biosensor chip. Importantly, since our method relies only on physical forces without any chemical treatment to refresh used receptor molecules, one can minimize possible contaminations and it can be applied for virtually-general receptor species. Furthermore, in our process, the magnetic nanobeads formed a single-layered film structure on the transducer surface, which allows one to apply our method to versatile biosensor devices including those which require receptors close to biosensor surfaces.

Figure 2(A) depicts the simulation results showing magnetic field strength around a nickel-based MRP structure when external magnetic fields were applied during the trapping and detrapping steps. Here, the simulation was performed using COMSOL multiphysics software. When a *strong* external magnetic field was applied with an upward direction, the MRP structure was magnetized along the external magnetic field direction (figure 2(A)(i)). In this case, the magnetic field by the magnetized MRP structure was added to the external magnetic field in the region just above the structure, resulting in a stronger magnetic field (brighter regions in figure 2(A)(i)) than that in other regions. Thus, we

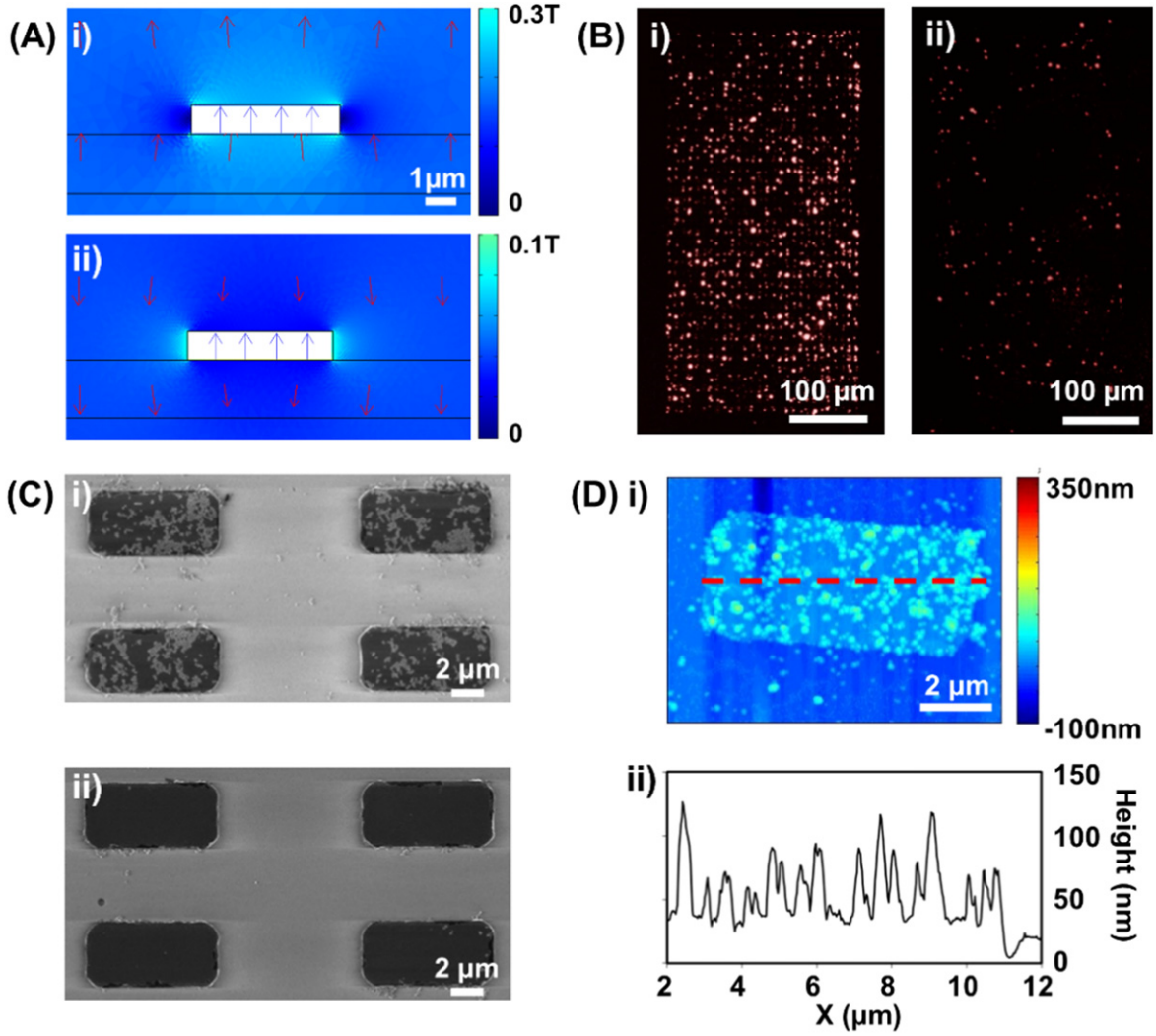

Figure 2. Trapping and detrapping of magnetic nanobeads on MRP structures. (A) Simulation results showing the cross-sectional view of a magnetic field strength around an MRP structure during (i) trapping and (ii) detrapping steps. *Brighter blue regions* and a *rectangle* represent the regions with *a stronger magnetic field* and an *MRP structure*, respectively. *Red* and *blue* arrows indicate the direction of the *magnetic fields* and the *magnetization of the MRP structure*, respectively. (B) Fluorescence images of MRP structures after (i) trapping and (ii) detrapping of fluorescence–labeled magnetic nanobeads. (C) SEM images of ferromagnetic MRP structures after (i) trapping and (ii) detrapping magnetic nanobeads. *Black rectangles and small gray circles* represent ferromagnetic *MRP structures* and *trapped magnetic nanobeads*, respectively. (D) (i) AFM image of MRP structures (rectangular bright region) after trapping magnetic nanobeads (small white dots) and (ii) height profiles along the dashed line in (i).

can expect that nearby superparamagnetic nanobeads can be attracted toward the MRP structure because magnetic dipoles are driven to the regions with a stronger magnetic field. Significantly, such a stronger magnetic field region extended only a very short distance from the MRP structure, which may enable the assembly of single-layered structures of the nanobeads. On the other hand, when a rather *weak* external magnetic field with a *reversed* direction was applied, the magnetization remained because of the magnetic hysteresis of the nickel-based MRP structure (figure 2(A)(ii)). In this case, the magnetic field by the MRP structure had an opposite direction to that of the external magnetic field, and, thus, the magnetic field just above the MRP structure became *weaker* (darker regions in figure 2(A)(i)) than in other regions. Here, we can expect that any superparamagnetic nanobeads on the MRP structure move away from the structure. These simulation results indicate that the hysteresis properties of ferromagnetic nickel-based MRP structures with a proper dimension can be utilized to exert *attractive* or *repulsive* forces to *trap* or *detrap* a precise amount of receptor-functionalized nanobeads down to a single-layer precision, respectively.

Figure 2(B) (*i*) and (*ii*) show the fluorescence images of the 30 × 28 array of nickel-based MRP structures after the *trapping* and *detrapping* of fluorescence-labeled magnetic nanobeads, respectively. The detailed procedure for trapping of the single-layered structures of nanobeads is presented in section 2. For the trapping of nanobeads, the external magnetic fields of 150 mT was applied in the direction perpendicular to the substrate surface. The fluorescence image shows well-ordered bright spots corresponding to the array of MRP structures, indicating a high yield of the magnetic

trapping process (figure 2(B)(i)). For the detrapping process, rather weak magnetic fields of 35 mT in the reversed direction was applied, and the solution on the substrate was replaced with PBS solution. The result shows that most of the nanobeads were removed from the substrate (figure 2(B)(ii)), indicating that the detrappng process can efficiently remove the nanobeads from the substrate. These results indicate that our method can be utilized to trap and detrap nanobeads over a large surface area with a high efficiency in real-time, which can be critical for practical applications. It also should be noted that this process can be performed without any chemical treatment, implying our method should be compatible with most receptor molecules for various biosensing applications.

Figure 2(C) (i) and (ii) show the field emission scanning electron microscope (SEM) images displaying the ferromagnetic nickel-based MRP structures (dark rectangular area) with nanobeads (white circular dots) after *trapping* and *detrapping* processes, respectively. After trapping and washing steps, magnetic nanobeads were found to form single-layered film structures on the MRP structures without being aggregated or stacked in a vertical direction (figure 2(C)(i)). Note that due to the residual magnetization of the ferromagnetic MRP structures, the magnetic nanobeads remained on the sensor surface even after removing external magnetic fields and washing the surface. Thus, one can take out the sensors with assembled nanobeads from the solution and use them for quite versatile applications and analyses such as SEM imaging and conventional sensing operations without external magnetic fields. The SEM images of assembled magnetic nanobeads after washing steps were analyzed to estimate the working area including the magnetic beads on the MRP structures, resulting in the working area value of $\sim$31% out of the entire MRP structure surface (supplementary data). Furthermore, from the surface area of an MRP structure and the measured number of antibody molecules on individual nanobeads, we can estimate that the number of antibody molecules on each MRP structure was $\sim 6.7 \times 10^4$ (supplementary data). After the detrapping process, most of the magnetic nanobeads were removed from the MRP structures, indicating the high efficiency of our trapping-detrapping method (figure 2(C)(ii)).

To confirm the formation of single-layered structures of nanobeads, the AFM characterization was performed (figure 2(D)). The AFM topography image shows that most of the nanobeads were trapped on the MRP structures and formed a layer with a rather uniform height (figure 2(D)(i)). The height profile along the red dashed line in the topography shows the height of the trapped nanobeads up to 50 nm, which corresponds to the hydrodynamic diameter of $\sim$100 nm (figure 2(D)(ii)) [28]. It supports the fact that the trapped nanobeads formed a monolayer structure without aggregation.

Figure 3(A) displays the operation of reusable fluorescence biosensors based on the MRP structures. Detailed processes are shown in section 2. In brief, ferromagnetic nickel-based MRP structures passivated with a PEG layer were fabricated via conventional microfabrication processes (figure 3(A)(i)). Here, the thin Au layer provided a stable surface without oxidation and, thus, enabled good interface with the biological solution, which can be very important for the sensing operation of some electrical sensors such as CNT transistor-based electrical sensors. Furthermore, as part of the fabrication process, we could apply well-known thiol chemistry to coat the Au surface with passivation molecules such as PEG, which prevented unwanted non-specific adsorption of biomolecules during the sensing operations. For a sensing operation, magnetic nanobeads functionalized with the 1st antibody were first assembled on the MRP structures by a rather strong magnetic field (figure 3(A)(ii)). After that, a target molecular species was applied so that target molecules could selectively bind to the complementary antibody on the nanobeads assembled on the ferromagnetic MRP structures (figure 3(A)(iii)). Finally, the 2nd antibody labeled with FITC was applied to the sensor, and the fluorescence from the 2nd antibody bound on the sensor surface was measured using a fluorescence microscope to confirm the selective sensing of the target molecular species (figure 3(A)(iv)). After the entire sensing processes, a rather weak magnetic field with a reversed direction was applied to remove the magnetic nanobeads, leaving a clean sensor surface for additional sensing operations. Note that since this process does not require any chemical process to refresh used sensors, it can be applied to virtually-general receptors for versatile biosensing applications.

Figure 3(B) shows the fluorescence images of three consecutive sensing experiments repeating the processes in figure 3(A). For the first complementary sensing experiment, nanobeads functionalized with the 1st antibody for IL-4 were assembled on the array of ferromagnetic MRP structures, and then a complementary target protein (IL-4, 57.1 pM in PBS solution) followed by the fluorescence-labeled complementary 2nd antibody were applied (figure 3(B)(i)). Note that the fluorescence image shows the array of fluorescent spots corresponding to the array of ferromagnetic structures, indicating the selective binding of complementary target molecules as well as the fluorescence-labeled 2nd antibody. This result clearly shows that the antibody molecules assembled onto the ferromagnetic MRP structures were working properly, and they can be utilized for selective biosensing applications. After the first experiment, the nanobeads were removed by applying a rather weak magnetic field with a reversed direction, and the *second* experiment with the same antibody for IL-4 and *non-complementary* target molecules (IL-10, 67.6 pM in PBS solution) were performed, resulting in low fluorescence signals (figure 3(B)(ii)). It indicates that the non-specific reaction in our sensor was very small. Furthermore, it should also be noted that the fluorescence signals in the first experiment (figure 3(B)(i)) actually came from the *fluorescence-labeled 2nd antibody bound to the 1st antibody with the complementary targets on the sensor surface*. Thus, the low fluorescence intensity after the second sensing experiment (figure 3(B)(ii)) implies the efficient removal of the antibodies used for the first experiment. After removing nanoparticles again, we performed the *third* experiment with the same antibodies and *complementary* targets (IL-4, 57.1 pM in PBS solution) on the same chip (figure 3(B) (iii)).

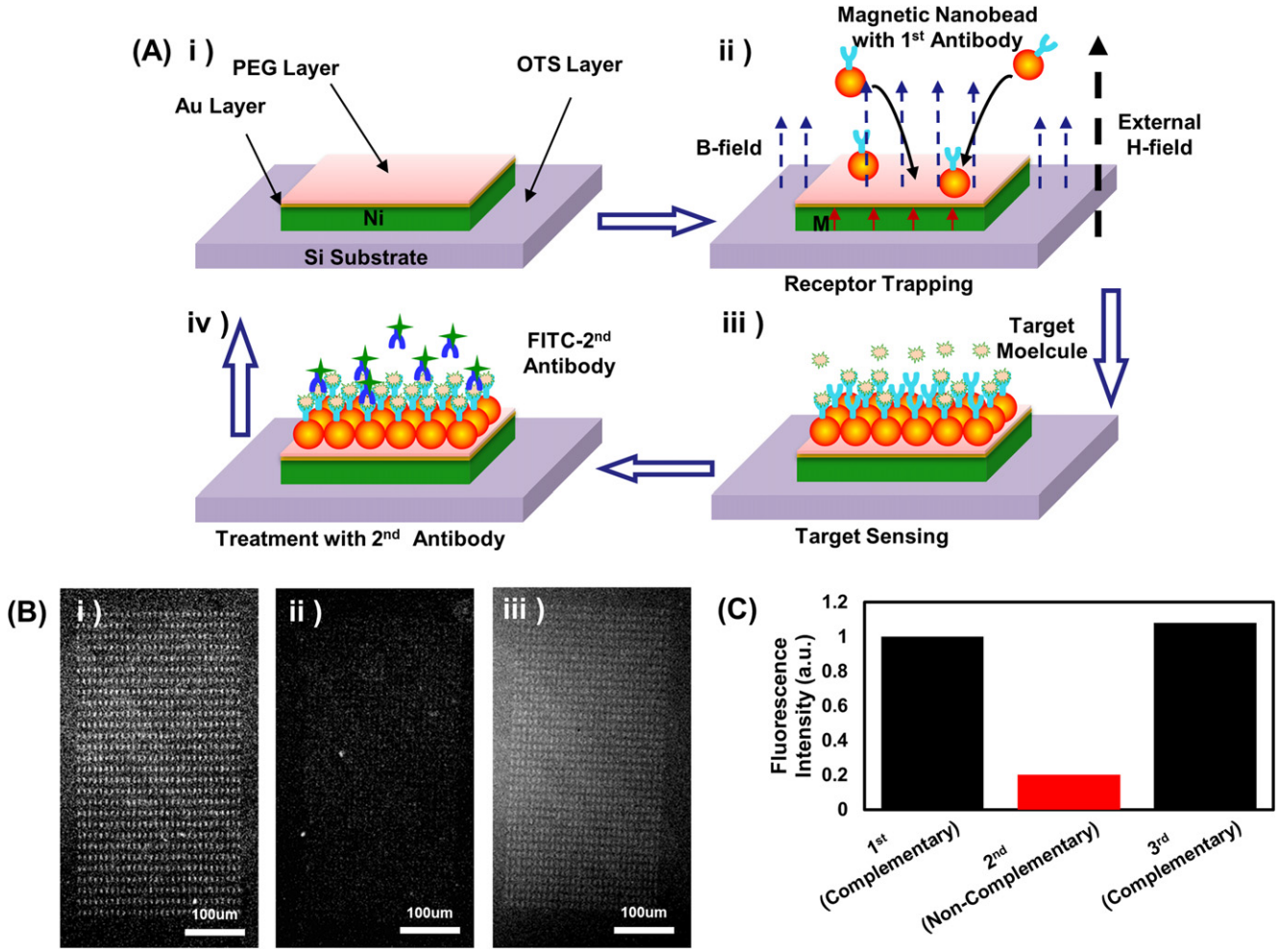

Figure 3. Reusable immunofluorescence sensors based on MRP structures. (A) A schematic diagram showing the repeated sensing operation of a fluorescence sensor based on the MRP structures. (B) (i) Fluorescence images after the first sensing test with IL-4 target molecules and corresponding *complementary* antibodies, (ii) the second sensing test with the same antibodies and *non-complementary* IL-10 target molecules, and (iii) the third sensing test with the same antibodies and the *complementary* IL-4 target molecules. Bright regions represent those with the IL-4 2nd antibody conjugated with fluorescent FITC dye. (C) Fluorescence intensity measured from the fluorescence images in (B).

Note that we can achieve the selective detection of target molecules again. These results clearly show that we can remove used receptors and repeatedly use a single chip for multiple sensing operations.

Figure 3(C) shows the graph of fluorescence intensity resulting from each sensing experiment. Note that the second sensing result using non-complementary target molecules exhibited quite a low fluorescence intensity, which means that the magnetic beads and their attached FITC molecules used in the first experiment were removed, and the non-complementary target molecule was not attached to the 1st antibody. On the other hand, the fluorescence intensity as a result of the third experiment using complementary target molecules recovered back to high intensity like that of the first complementary sensing experiment. These results clearly show that the reusable fluorescence sensors based on our MRP structure can be utilized repeatedly while maintaining their high selectivity and sensitivity.

Figure 4(A) illustrates the schematic diagram for the repeated sensing operations of a reusable CNT transistor-based electrical biosensor. The detailed procedure is presented in section 2. In brief, a CNT transistor device with floating electrodes was first fabricated as reported previously (figure 4(A)(i)) [27]. This device is comprised of a CNT network channel connecting source and drain electrodes with fixed bias voltage and floating electrodes in the middle of the CNT channel. Here, the MRP structure based on nickel was integrated as part of the floating electrode. In this sensor, the selective binding of biomolecules to receptor molecules on the floating electrode surface altered the work function of the Au electrode and, eventually, changed the electrical currents in the CNT transistor. Thus, one can detect the target molecules simply by monitoring the electrical current change in the transistor device. Note that since this CNT transistor-based sensor responds to target molecules only within the Debye length distance from the floating electrode surface, it is

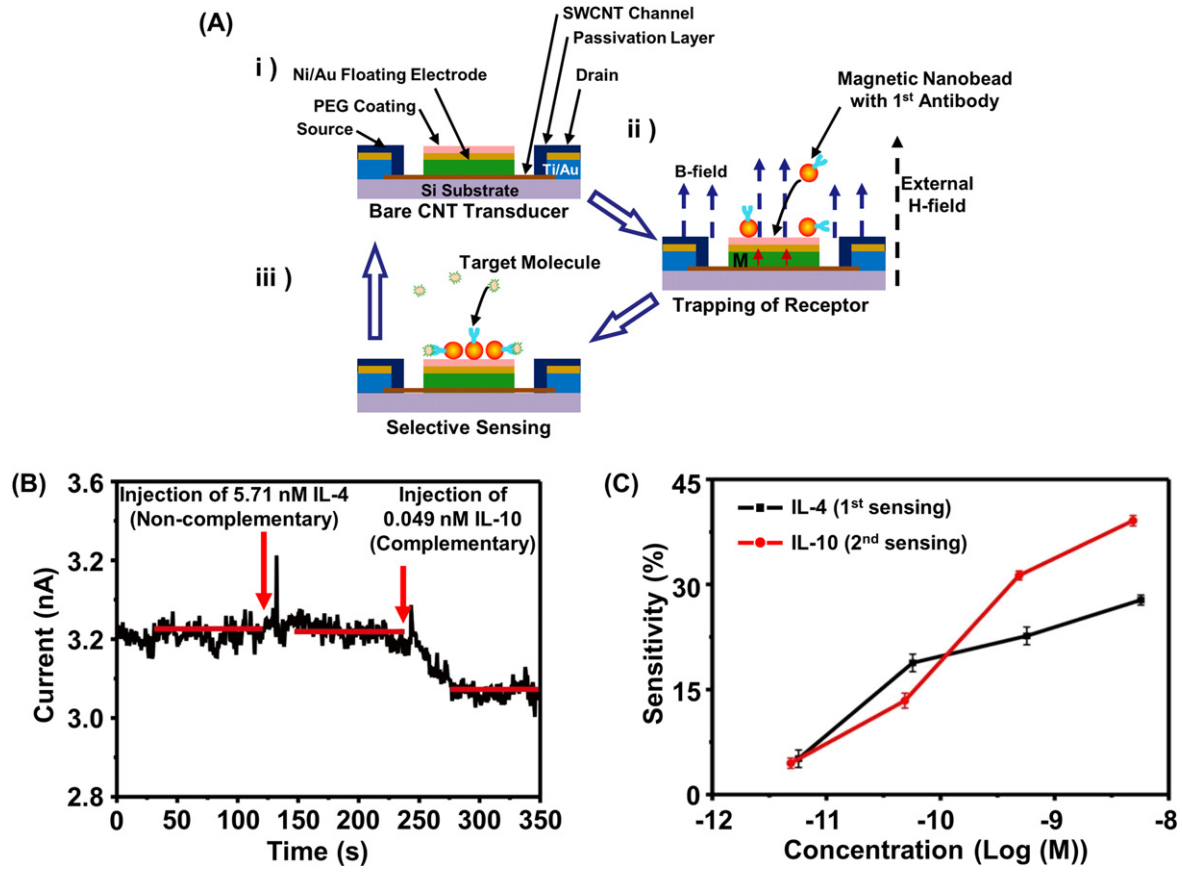

Figure 4. Reusable CNT transistor-based biosensors based on MRP structures. (A) A schematic diagram showing the repeated sensing cycle of a reusable CNT transistor-based electrical biosensor; (i) CNT transistor comprised of CNT network channels between source and drain electrodes with fixed bias voltages and floating electrodes based on Ni, (ii) assembly of nanobeads functionalized with 1st antibody onto the floating electrodes via external magnetic fields, (iii) sensing of target molecules. (B) Real-time sensor responses after the introduction of IL-4 and IL-10 target proteins to a CNT transistor-based sensor including assembled nanobeads functionalized with IL-10 antibody. (C) Sensing of two different target molecules (IL-4 and IL-10) by repeating the sensing experiments using nanobeads functionalized with two different antibodies.

critical to place the receptor molecules close to the electrode surface. For a sensing operation, the solution of the 1st antibody-functionalized nanobeads was applied to the CNT transistor, and an external magnetic field was applied so that the nanobeads in the solution were assembled on the floating electrodes with the nickel-based MRP structure (figure 4(A)(ii)). After trapping the nanobeads, the magnetic field was removed so that it did not disturb the CNT transistor during the sensing operations. Note that due to the residual magnetization of ferromagnetic MRP structures, the magnetic nanobeads remained on the sensor surface even after removing the external magnetic fields. It should be mentioned that in previous methods using only external magnetic fields without ferromagnetic patterns, rather strong external magnetic fields were usually required to hold stable amounts of magnetic beads on the sensor surface, which could generate electrical noises and disturb the operation of highly-sensitive nano-biosensors [20, 24]. When the solution of target molecules was applied, the target molecules selectively bound to the antibody on the assembled nanobeads and, eventually, altered the electrical currents in the CNT transistor device, which was utilized as a sensing signal (figure 4(A)(iii)). Significantly, in our method, nanobeads formed a single-layered structure on the floating electrodes so that antibody molecules on the assembled nanobeads were within a Debye length from the electrode surface and the sensor could detect the selective binding of target molecules onto the receptor molecules. After the sensing step, the nanobeads can be removed simply by applying a rather weak magnetic field with a reversed direction, leaving a clean floating electrode surface for additional sensing operations. It should be mentioned that since the used antibody on the sensor surface can be refreshed simply by adjusting external magnetic fields without relying on chemical processes, this process can be applied for versatile sensors based on virtually-general receptor molecular species.

Figure 4(B) shows the real-time response of a reusable CNT transistor-based sensor based on MRP structures by the addition of non-complementary (IL-4) and complementary (IL-10) biomolecular species. Here, nanobeads with an IL-10 antibody were first trapped on the Ni/Au floating electrode surface, and a 5.71 nM of non-complementary biomolecular (IL-4) solution and a 0.049 nM of complementary biomolecular (IL-10) solution were applied in sequence while

monitoring the electrical currents between the source and drain electrodes. Note that the electrical currents did not change by the addition of non-complementary IL-4 molecules, while the addition of the complementary IL-10 molecular species resulted in the clear change of electrical currents. This result clearly shows that the receptors on the trapped nanobeads functioned properly, and our sensors selectively detect the target molecules. Previous works show that some biosensors such as transistor-type or surface plasmon resonance-based biosensors can detect target molecules only within a short distance from the device surface [25, 26]. Since, in our method, the nanobeads with receptors formed a single-layered structure on our device surface, the receptors can be placed within a short distance from the device surface, enabling the sensing operation of such sensors. Thus, the formation of single-layered film structures of nanobeads in our method can be a significant advantage in building reusable sensors based on such sensor transducer devices [27, 29].

Since our method allows one to repeatedly functionalize and refresh receptor molecules on a device surface, we could easily functionalize a single CNT transistor device with different receptor molecules and use it to detect different target molecules (figure 4(C)). In this experiment, nanobeads with an IL-4 antibody were first assembled on a CNT transistor device, and the device was utilized to detect IL-4 with different concentrations from 100 pg ml^{-1} to 100 ng ml^{-1} (black dots in figure 4(C)). The nanobeads with used antibody could be removed by applying external magnetic fields with a reversed direction. Later, nanobeads functionalized with the IL-10 antibody were assembled again onto the floating electrode surface, and the sensing experiment using an IL-10 molecular solution was performed (red dots in figure 4(C)). The results show the increasing response of our sensors with increasing target molecular concentrations. The graphs were fitted using the equation based on the Langmuir isotherm model as reported previously [27]. From the fitting, we can estimate the equilibrium constant of IL-4 and IL-10 as $3.36 \times 10^{10}\,M^{-1}$ and $5.08 \times 10^{10}\,M^{-1}$, respectively. These values are in the same order as those reported previously [30]. These results show that our MRP structure allowed one to use a single transducer device for the detection of different molecular species, which clearly shows the versatility and effectiveness of our method.

4. Conclusions

In conclusion, we developed the MRP structure which can be integrated with versatile nanodevice-based sensor transducers to build reusable biosensors based on virtually-general receptor molecules. The magnetic hysteresis properties of the ferromagnetic MRP structures integrated as a part of a nano-biosensor were utilized to trap or remove magnetic nanobeads with receptor molecules on the nano-biosensor device for repeated sensing operations. Using the MRP structure, we demonstrated the repeated sensing operations of fluorescence biosensors and CNT transistor-based electrical biosensors. Significantly, since entire multiple biosensing operations can be done simply by adjusting external magnetic fields without using any harsh chemical treatment, this MRP structure can be applied to versatile biosensors based on virtually-general receptor molecules. Furthermore, this method allows one to assemble a single-layered film structure of receptor-functionalized nanobeads on the biosensor surface so that an active antibody can be placed within a very short distance from the biosensor surface. Thus, this MRP structure can be utilized for some biosensors (e.g. transistor-type, surface plasmon resonance-based) which require receptor molecules very close to the sensor surface. We also demonstrated the detection of two different target molecular species using only a single CNT transistor-based biosensor chip. Our method is a simple but powerful strategy which allows one to reuse rather expensive nano-biosensor devices and, eventually, bring them for practical applications. In addition, it may pave the way toward advanced biosensing applications such as a real-time monitoring system of hazardous viruses in public places.

Acknowledgments

This work was supported by BioNano Health-Guard Research Center funded by the Ministry of Science, ICT & Future Planning (MSIP) of Korea as Global Frontier Project (No. H-GUARD_2013M3A6B2078961). SH also acknowledges the support from NRF grants (Nos. 2013M3C8A3078813, 2015M3C1A3002152).

References

[1] Hansen J A, Sumbayev V V and Gothelf K V 2007 An electrochemical sensor based on the human estrogen receptor ligand binding domain *Nano Lett.* **7** 2831–4
[2] Ko J W, Woo J-M, Jinhong A, Cheon J H, Lim J H, Kim S H, Chun H, Kim E and Park Y J 2011 Multi-order dynamic range DNA sensor using a gold decorated SWCNT random network *ACS Nano* **5** 4365–72
[3] Inci F, Tokel O, Wang S, Gurkan U A, Tasoglu S, Kuritzkes D R and Demirci U 2013 Nanoplasmonic quantitative detection of intact viruses from unprocessed whole blood *ACS Nano* **7** 4733–45
[4] Farrow B *et al* 2013 A chemically synthesized capture agent enables the selective, sensitive, and robust electrochemical detection of anthrax protective antigen *ACS Nano* **7** 9452–60
[5] Lo Y-S, Nam D H, So H-M, Chang H, Kim J-J, Kim Y H and Lee J-O 2009 Oriented immobilization of antibody fragments on Ni-decorated single-walled carbon nanotube devices *ACS Nano* **3** 3649–55
[6] Zhang T, He Y, Wei J and Que L 2012 Nanostructured optical microchips for cancer biomarker detection *Biosens. Bioelectron.* **38** 382–8
[7] Alwarappan S, Erdem A, Liu C and Li C-Z 2009 Probing the electrochemical properties of graphene nanosheets for biosensing applications *J. Phys. Chem.* C **113** 8853–7
[8] Alwarappan S, Liu G and Li C-Z Simultaneous detection of dopamine, ascorbic acid, and uric acid at electrochemically

pretreated carbon nanotube biosensors nanomed *Nanotechnol. Biol. Med.* **6** 52–7
[9] Mishra M, Alwarappan S, Joshi R K and Mohanty T 2013 Chemically synthesized graphene for electrochemical biosensing *J. Nanosci. Nanotechnol.* **13** 4040–4
[10] Liu Y, Yu X, Zhao R, Shangguan D-H, Bo Z and Liu G 2003 Quartz crystal biosensor for real-time monitoring of molecular recognition between protein and small molecular medicinal agents *Biosens. Bioelectron.* **19** 9–19
[11] An J H, Park S J, Kwon O S, Bae J and Jang J 2013 High-performance flexible graphene aptasensor for mercury detection in mussels *ACS Nano* **7** 10563–71
[12] Radke S M and Alocilja E C 2005 A microfabricated biosensor for detecting foodborne bioterrorism agents *IEEE Sensors J.* **5** 744–50
[13] Chen X, Kim D and Hong S 2014 The carbon nanotube-based nanobiosensor: a key component for ubiquitous real-time bioscreening system? *Nanomedicine* **9** 565–7
[14] Yeh P-H, Li Z and Wang Z L 2009 Schottky-gated probe-free ZnO nanowire biosensor *Adv. Mater.* **21** 4975–8
[15] Baselt D R, Lee G U, Natesan M, Metzger S W, Sheehan P E and Colton R J 1998 A biosensor based on magnetoresistance technology1 *Biosens. Bioelectron.* **13** 731–9
[16] Sosa N E, Chen C, Liu J, Xie S, Marks T J and Hersam M C 2010 Nanoscale structure, composition, and charge transport analysis of transparent conducting oxide nanowires written by focused ion beam implantation *J. Am. Chem. Soc.* **132** 7347–54
[17] Li W-S, Hou P-X, Liu C, Sun D-M, Yuan J, Zhao S-Y, Yin L-C, Cong H and Cheng H-M 2013 High-quality, highly concentrated semiconducting single-wall carbon nanotubes for use in field effect transistors and biosensors *ACS Nano* **7** 6831–9
[18] Sapsford K E, Shubin Y S, Delehanty J B, Golden J P, Taitt C R, Shriver-Lake L C and Ligler F S 2004 Fluorescence-based array biosensors for detection of biohazards *J. Appl. Microbiol.* **96** 47–58
[19] Asada H H, Shaltis P, Reisner A, Sokwoo R and Hutchinson R C 2003 Mobile monitoring with wearable photoplethysmographic biosensors *IEEE Eng. Med. Biol. Mag.* **22** 28–40
[20] Sun Y, Bai Y, Song D, Li X, Wang L and Zhang H 2007 Design and performances of immunoassay based on SPR biosensor with magnetic microbeads *Biosens. Bioelectron.* **23** 473–8
[21] Wang D, Chen G, Wang H, Tang W, Pan W, Li N and Liu F 2013 A reusable quartz crystal microbalance biosensor for highly specific detection of single-base DNA mutation *Biosens. Bioelectron.* **48** 276–80
[22] Gijs M M 2004 Magnetic bead handling on-chip: new opportunities for analytical applications *Microfluid. Nanofluid.* **1** 22–40
[23] Xu Y and Wang E 2012 Electrochemical biosensors based on magnetic micro/nano particles *Electrochim. Acta* **84** 62–73
[24] Zhu D, Liu J, Tang Y and Xing D 2010 A reusable DNA biosensor for the detection of genetically modified organism using magnetic bead-based electrochemiluminescence *Sensors Actuators B* **149** 221–5
[25] Ohno Y, Maehashi K and Matsumoto K 2010 Label-free biosensors based on aptamer-modified graphene field-effect transistors *J. Am. Chem. Soc.* **132** 18012–3
[26] Heller I, Chatoor S, Männik J, Zevenbergen M A G, Dekker C and Lemay S G 2010 Influence of electrolyte composition on liquid-gated carbon nanotube and graphene transistors *J. Am. Chem. Soc.* **132** 17149–56
[27] Kim B, Lee J, Namgung S, Kim J, Park J Y, Lee M-S and Hong S 2012 DNA sensors based on CNT-FET with floating electrodes *Sensors Actuators B* **169** 182–7
[28] Kim E, Oh J-S, Ahn I-S, Park K I and Jang J-H 2011 Magnetically enhanced adeno-associated viral vector delivery for human neural stem cell infection *Biomaterials* **32** 8654–62
[29] Homola J 2003 Present and future of surface plasmon resonance biosensors *Anal. Bioanal. Chem.* **377** 528–39
[30] Junttila I S, Mizukami K, Dickensheets H, Meier-Schellersheim M, Yamane H, Donnelly R P and Paul W E 2008 Tuning sensitivity to IL-4 and IL-13: differential expression of IL-4Rα, IL-13Rα1, and γc regulates relative cytokine sensitivity *J. Exp. Med.* **205** 2595–608